UNCLASSIFIED

AD **4 4 4 3 4 3**

DEFENSE DOCUMENTATION CENTER

FOR

SCIENTIFIC AND TECHNICAL INFORMATION

CAMERON STATION, ALEXANDRIA, VIRGINIA

UNCLASSIFIED

PICATINNY ARSENAL TECHNICAL REPORT 3153

RATES OF IONIZATION AND
RECOMBINATION PROCESSES IN HEATED AIR

1ST LT. JAMES H. RENKEN

JULY 1964

AMCMS CODE 5910.21.830.29

DDC

AUG 19 1964

DDC-IRA C

PICATINNY ARSENAL
DOVER, NEW JERSEY

The findings in this Report are not to be construed as
an official Department of the Army position.

DISPOSITION

Destroy this report when it is no longer needed.
Do not return.

DDC AVAILABILITY NOTICE

Qualified requesters may obtain copies of this report
from DDC.

RATES OF IONIZATION AND
RECOMBINATION PROCESSES IN HEATED AIR

by

1st Lt. James H. Renken

July 1964

Feltman Research Laboratories
Picatinny Arsenal
Dover, N. J.

Technical Report 3153

AMCMS Code 5910.21.830.29

Approved:
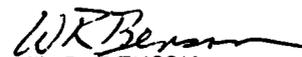
W. R. BENSON
Chief, Engineering
Sciences Laboratory

FOREWORD

This report presents results of one phase of the work in progress at
Picatinny Arsenal on the DASA NWER Subtask 08.008 Integrated Effects
program.

TABLE OF CONTENTS

TABLE OF CONTENTS (cont)

Page

SUMMARY

The procedures used to calculate rate constants for certain ionization and recombination reactions have been described. Results of calculations based upon these procedures and analytical expressions which approximate the values found with the computer have been presented.

The only recombination reactions which have been treated are those which yield a hydrogenic ion. Extension of the present formalism to cases where multi-electron ions are formed is restricted primarily by the lack of convenient radiative transition rate information for multi-electron systems.

1

INTRODUCTION

Many of the properties of a plasma depend upon the concentrations of the constituent ionic species and the relative population of the energy levels of each ionization state. In situations where thermodynamic equilibrium can be assumed to exist, such parameters are characterized by a temperature and can be found most easily by using the Saha ionization formula and the well known Boltzmann formula. The use of these formulas results in simplification in any analysis because a detailed examination of the many processes which lead to excited-state and ionic-state equilibrium concentrations is not required.

In situations where thermodynamic equilibrium cannot be assumed, it is necessary to enumerate the processes which cause ionization, recombination, and excitation, and then to determine the relative probability of each. Depending upon the number of transitions permitted by the selection rules, this can be a formidable task. In practice, it is usually necessary to pick a few transitions which, hopefully, will dominate the others. If this simplification is valid, then calculations using the dominant transitions will adequately describe the actual physical situation.

When calculations are done to describe certain aspects of nuclear weapon phenomenology, situations are encountered where a large amount of electromagnetic energy is deposited in the atmosphere during a very short time interval. In order to utilize the various rate equations which govern the ionic concentrations, it is necessary to determine the transition coefficients for several reactions which appear to dominate the physical situation. The following sections present results of calculations to determine rate coefficients for three types of atomic reactions: electron-impact ionization, three-body recombination, and radiative recombination.

ELECTRON-IMPACT IONIZATION

Definition of the Process

In a plasma composed of atoms and free electrons having substantial kinetic energy, it is quite conceivable that a free electron may, through the Coulomb interaction, transfer a fraction of its energy sufficient to liberate a bound electron. This process can be represented symbolically by

$$X + e^- \rightarrow X^+ + 2\,e^-$$

2
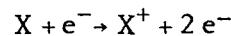
where X is any neutral or partially stripped atom. This expression will be taken as the definition of the electron-impact ionization process. It should be noted that the final state for this reaction has two free electrons. Exchange-type collisions were the initially bound electron is freed and the incident electron is captured will occur, but such a process is unimportant when ways of changing the degree of ionization of the plasma are being considered.

Theoretical Reaction Cross Sections

Although quantum mechanical techniques for finding the cross section for the reaction under consideration are available, the effort required to obtain a solution for any but, say, one-electron or two-electron target atoms would be very great. Since information concerning reaction rates in air is desired, the use of extensive quantum mechanical calculations to determine the required cross sections is clearly impracticable.

Values for the cross sections used in this study were calculated using the semiclassical theory of Gryziński (Ref 1). To summarize this theory, consider the interaction of two particles having charges q_1 and q_2, masses m_1 and m_2, and velocities v_1 and v_2, respectively. Let ΔE be the change in energy of particle 2, which is assumed to be the incoming particle, and let E_1 and E_2 be the energies of particles 1 and 2 before the collision. Then Gryziński writes the cross section for a collision in which the incoming particle suffers an energy loss greater than U as

$$Q(U) = \int_U^{\Delta E_{max}} \sigma(\Delta E) \, d(\Delta E)$$

where $\sigma(\Delta E)$ is the cross section for an encounter in which an amount of energy ΔE is lost by particle 2. When $m_1 \cong m_2$,

$$Q(U) = \frac{\sigma_0}{U^2} g\left[\frac{E_2}{U}; \frac{E_1}{U}\right] \tag{1}$$

3

where

$$g\left[\frac{E_2}{U}; \frac{E_1}{U}\right] = \left(\frac{V_2^2}{V_2^2 + V_1^2}\right)^{3/2} \times$$

$$\frac{2}{3}\frac{E_1}{E_2} + \frac{U}{E_2}\left(1 - \frac{E_1}{E_2}\right) - \left(\frac{U}{E_2}\right)^2, \text{ if } U + E_1 \leq E_2 \qquad (2)$$

$$\frac{2}{3}\left[\frac{E_1}{E_2} + \frac{U}{E_2}\left(1 - \frac{E_1}{E_2}\right) - \left(\frac{U}{E_2}\right)^2\right]\left[\left(1 + \frac{U}{E_1}\right)\left(1 - \frac{U}{E_2}\right)\right]^{1/2}, \text{ if } U + E_1 \geq E_2$$

and for electrons interacting with electrons

$$\sigma_0 = \pi \, \epsilon^4 = 6.511 \times 10^{-14} \text{ cm}^2 \text{ eV}^2.$$

Let the velocity distribution of the j-shell electrons in an atom be denoted by $N^{(j)}(v_1)$ and their ionization potential by $U^{(j)}$. Then the value of the cross section for electron-impact ionization can be written as

$$\sigma_i = \sum_j \int_0^\infty N^{(j)}(v_1) \, Q \, (U^{(j)}) \, dv_1 \qquad (3)$$

where the minimum energy transfer has been set equal to the ionization potential. Gryziński obtains good results by using a δ-function for the bound-electron velocity distribution. Thus, for example, when considering a helium target, $N_{He}(v_1) = 2 \, \delta \, [v_1 - (2E_1/m_e)^{1/2}]$ where E_1 is constant. Although Equation 3 formally contains a sum over various electron shells, the occurrence of the factor U^{-2} in Equation 1 means that removal of K-shell electrons will be insignificant compared with removal of P-shell electrons because of the much higher ionization potential of the former.

Parameters for Specific Ions

In order to calculate values for the ionization cross sections using the semiclassical theory, it is necessary to know the kinetic energy of the P-shell electrons and their ionization potentials. The latter are easily obtained from Moore's work (Ref 2) but the kinetic energies can only be estimated.

4

In keeping with the spirit of the semiclassical approach, it is assumed that all the P-shell electrons of a given ion move in the same circular orbit about the charged nucleus. With this approximation, the potential energy of the electrons is given by $V = -Z^*\epsilon^2/r_2$ where $Z^*\epsilon$ is the effective nuclear charge and r_2 is the radius of the orbit for the principal quantum number of $m = 2$. This radius is obtained from $r_m = m^2 a_o/Z^*$ where a_o is the Bohr radius. Using the shielding factors given by Slater (Ref 3), reasonable estimates of the effective charges can be found for the ions considered here. Since

$$\text{Kinetic energy} + \text{ionization potential} = |V|,$$

it is possible to estimate the kinetic energy of the P-shell electrons. By using this technique, the values listed in Table 1 are found.

TABLE 1

Parameters characterizing the motion of P-shell electrons in nitrogen and oxygen ions

Ion	Ionization Potential	Z^*	E_1
N I	14.54 eV	3.90	89.0 eV
N II	29.61	4.25	93.3
N III	47.43	4.60	96.6
N IV	77.45	4.95	89.3
N V	97.86	5.30	93.3
O I	14.61 eV	4.55	127.3 eV
O II	35.13	4.90	128.3
O III	54.93	5.25	132.7
O IV	77.39	5.60	136.0
O V	113.87	5.95	127.0
O VI	138.08	6.30	132.0

Comparison with Quantum Mechanical and Experimental Cross Section Values

Trefftz (Ref 4) gives the results obtained from quantum mechanical calculations of the ionization cross section when electrons are indident on O^{4+} (OV) and O^{5+} (OVI). The results are

5

$$\sigma_i^{qm}(O^{4+}) = 2.42 \times 10^{-18} \text{ cm}^2$$

when $E_2 = 261$ eV for the ionization of O^{4+} and

$$\sigma_i^{qm}(O^{5+}) = 0.86 \times 10^{-18} \text{ cm}^2$$

when $E_2 = 255$ eV for the ionization of O^{5+}.

By using Equations 1, 2, and 3, and the parameters shown in Table 1 with the assumption that the minimum energy transfer U equals the ionization potential, the semiclassical cross section for ionization of O^{4+} is found to be

$$\sigma_i^{sc}(O^{4+}) = 2.00 \times 10^{-18} \text{ cm}^2.$$

Similarly, for the ionization of O^{5+}, the semiclassical result is found to be

$$\sigma_i^{sc}(O^{5+}) = 0.57 \times 10^{-18} \text{ cm}^2.$$

Considering the complexity of the problem and the simplifying assumptions which are required with each approach, the agreement of these results is quite satisfactory.

In addition to the quantum mechanical results, a limited amount of experimental data is available. Fite and Brackman (Ref 5) have measured the cross section for the reaction

$$O + e^- \rightarrow O^+ + 2e^-$$
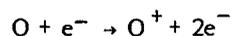
and Seaton (Ref 6) has derived cross section values for

$$N + e^- \rightarrow N^+ + 2e^-$$
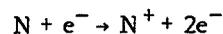
from other experimental data. Figures 1 and 2 (pp 24 and 25) show these relationships and the comparable semiclassical calculations. It can be seen that the calculated results are two to four times as large as the experimental results, but the shape of the calculated curves, when properly normalized, agrees fairly well with experiment. The only parameter in the theory about which any appreciable uncertainty exists is the kinetic energy

6

of the bound electrons E_i. Points are plotted in Figure 1 for calculations done with E_i = 100 eV and 150 eV, and it can be seen that changes in E_i do not appreciably alter the threshold behavior of the calculated cross section.

The Reaction Rate

The reaction rate is expressed in terms of the reaction cross section by the relation

$$\text{Rate} = \int_0^\infty \int_0^\infty \sigma \left(|\underline{v}_2 - \underline{v}_i| \right) \ |\underline{v}_2 - \underline{v}_i| \ F(\underline{v}_2) \, d\underline{v}_2 \ G(\underline{v}_i) \, d\underline{v}_i \qquad (4)$$

where $F(\underline{v}_2)$ and $G(\underline{v}_i)$ are the distribution functions for the velocity of the incident electrons and the target ions, respectively. Because of the large mass difference between an ion and an electron, however, the motion of an ion in a fixed coordinate system compared to that of a free electron is negligible. This does not mean that the initial velocity of the bound electron which is liberated during the encounter with the free electron is negligible compared to the latter's velocity. In fact, consideration of the relative motion of the bound and free electrons is included by Gryziński in the development of the theory described previously.

When the velocity of the target ions is disregarded, the reaction rate can be expressed by

$$\text{Rate} = \int_0^\infty G(v_i) \, dv_i \int_0^\infty \sigma(v_2) v_2 \ F(v_2) \, dv_2$$

$$= n_i \, n_e \int_0^\infty \sigma(v_2) \ v_2 \ f(v_2) \, dv_2 \qquad (5)$$

where f is the normalized velocity distribution function and n_i and n_e are the ion and free electron concentrations, respectively. Equation 5 can also be written in the form

$$\frac{dn_i}{dt} = - \alpha n_i n_e$$

where the rate coefficient α is defined by

$$\alpha = \int_0^\infty \sigma(v_2) \ v_2 \ f(v_2) \, dv_2 \qquad (6)$$

7

The question of what the exact form of the distribution function f is cannot be answered in general. However, estimates using expressions given by Spitzer (Ref 7) for the time required for nonequilibrium gases to attain equilibrium indicate that, with reasonable particle concentrations, the Maxwellian velocity distribution is reached very quickly. Hence, for convenience and for the lack of any better distribution, the free electron velocity distribution is assumed to be Maxwellian.

After changing the integration variable in Equation 6 from velocity to energy, and using Equation 3, the rate coefficient can be written in the form

$$\alpha = \kappa \ (I_1 + I_2).$$

Here

$$\kappa = \left(\frac{1}{\pi \ m_e \ c^2}\right)^{1/2}\left(\frac{2}{kT}\right)^{3/2} \frac{\sigma_o \ N_j \ c}{U^2} \qquad (7)$$

where N_j is the number of bound electrons of the type being removed, c is the speed of light, m_e is the electron mass, k is the Boltzmann constant, and T is the temperature characterizing the free electron distribution. The symbols I_1 and I_2 denote the integrals

$$I_1 = \frac{2}{3}\int_U^{U+E_1} \left(\frac{E_2}{E_1 + E_2}\right)^{3/2}\left[\left(1 + \frac{U}{E_1}\right)\left(1 - \frac{U}{E_2}\right)\right]^{1/2} \left[\left(E_1 + U\right) - \frac{U}{E_2}\left(E_1 + U\right)\right]e^{-\frac{E_2}{kt}} dE_2$$

$$\qquad (8)$$

$$I_2 = \int_{U+E_1}^{\infty} \left(\frac{E_2}{E_1 + E_2}\right)^{3/2} \left[\frac{2}{3} E_1 + U - \frac{U}{E_2}\left(E_1 + U\right)\right]e^{-\frac{E_2}{kT}}dE_2 \qquad (9)$$

These integrals seem to be intractable analytically. This difficulty is due to the terms with the fractional exponents. The energy dependence of these terms is shown in Figure 3 (p 26) for a typical ion. The results, shown in Figure 3, suggest that polynomials of the second degree can be used to replace the "troublesome" factors in Equations 8 and 9. Hence, for the sake of obtaining analytical result for the rate coefficient it is assumed that

$$\left(\frac{E_2}{E_2 + E_1}\right)^{3/2} \left[\left(1 + \frac{U}{E_1}\right)\left(1 - \frac{U}{E_2}\right)\right]^{1/2} \rightarrow AE_2^2 + BE_2 + C; \ U \le E_2 \le U + E_1$$

8

$$\left(\frac{E_2}{E_2 + E_1}\right)^{3/2} \rightarrow DE_2^2 + EE_2 + F; \quad U + E_1 \leq E_2 \leq 100\,E_1$$

$$\left(\frac{E_2}{E_2 + E_1}\right)^{3/2} \rightarrow 1; \quad E_2 < 100\,E_1$$

where the constants A, B, C, D, E, and F are to be determined by fitting the polynomials to the expressions which they replace.

After introducing this simplification, performing the integrations, and making the substitutions

$$V = (2/3)\,E_1 + U$$

$$W = E_1 + U$$

$$X = U/kT$$

$$Y = (E_1 + U)/kT$$

$$R = 100\,E_1/kT,$$

I_1 and I_2 are given by

$$I_1 = \frac{2}{3}\,W\,(kT)^3\,A\{\exp(-X)\,[X^2 + 2X + 2] - \exp(-Y)\,[Y^2 + 2Y + 2]\}$$

$$+ \frac{2}{3}\,W\,(B\text{-}AU)\,(kT)^2\,\{\exp(-X)\,[X+1] - \exp(-Y)\,[Y+1]\} \tag{10}$$

$$+ \frac{2}{3}\,W\,(C\text{-}BU)\,kT\,[\exp(-X) - \exp(-Y)]$$

$$+ \frac{2}{3}\,WCU\,[Ei(-X) - Ei(-Y)]$$

and

$$I_2 = V\,(kT)^3\,D\{\exp(-Y)\,[Y^2 + 2Y + 2] - \exp(-R)\,[R^2 + 2R + 2]\}$$

$$+ [VE\text{-}WDU]\,(kT)^2\,\{\exp(-Y)\,[Y+1] - \exp(-R)\,[R+1]\}$$

$$\tag{11}$$

$$+ [VF\text{-}WEU]\,(kT)\,[\exp(-Y) - \exp(-R)]$$

$$+ WU\,[F\,Ei(-Y) + (1\text{-}F)\,Ei(-R)] + V\,kT\,\exp(-R)$$

9

where

$$-\text{Ei}\,(-X) = \int_X^\infty \frac{e^{-t}}{t}\,dt\,.$$

The Rate Coefficient Calculation

A computer program for the IBM 709 was written to determine the polynomial constants and to evaluate the rate coefficient using Equations 7, 10, and 11, and the parameters listed in Table 1 (p 5). In order to improve the accuracy of the calculated results, the theoretical cross sections for all oxygen and nitrogen ions were multiplied by the "normalization factors" required to improve agreement between the O I and N I theoretical and experimental cross sections, respectively. Unfortunately, the experimental data available is not sufficient for determining individual normalization factors for each type of ion. Hence it is necessary to use the O I normalization factor for all oxygen ion calculations and the N I normalization factor for all nitrogen ion calculations

To determine the polynomial fitting constants, the end points and a point near the center of the curve being approximated were used as the three fitting points. Comparison of the polynomial expressions with the exact functions indicated that the agreement between the two functions was generally within 20% throughout the range of validity.

The calculated rate coefficients are shown in Figures 4 and 5 (pp 27 and 28). To facilitate the use of these results in digital computer calculations, the rate coefficients shown in these figures were approximated by expressions of the form

$$G\,T^n\,(1 + HT).$$

Table 2 (p 11) gives the appropriate values of G, H, and n in the indicated temperature ranges. Values calculated with these simplified expressions are for the most part within 5% of the computer results.

10

TABLE 2

Fit coefficients for simplified rate coefficient expressions

Ion	Temperature Range	n	G	H
N I	1.95 (4)* to 2.50 (4)	9	1.8556 (−51)	1.6510 (−5)
	2.50 (4) to 3.50 (4)	6	7.3622 (−39)	1.8254 (−4)
	3.50 (4) to 5.60 (4)	4	8.2322 (−30)	2.0271 (−4)
	5.60 (4) to 1.20 (5)	3	5.6130 (−24)	2.5831 (−7)
	1.20 (5) to 2.00 (5)	1	2.0833 (−14)	2.5000 (−5)
	2.00 (5) to 3.50 (5)	1	1.0119 (−13)	1.1765 (−6)
	3.50 (5) to 1.00 (6)	0	2.7385 (− 8)	2.3600 (−6)
N II	4.00 (4) to 5.80 (4)	6	2.0294 (−40)	5.0762 (−6)
	5.80 (4) to 8.70 (4)	5	5.5801 (−36)	2.9833 (−5)
	8.70 (4) to 1.55 (5)	3	2.5805 (−27)	6.6492 (−4)
	1.55 (5) to 2.00 (5)	2	1.2770 (−20)	1.4577 (−5)
	2.00 (5) to 3.00 (5)	2	4.5556 (−20)	4.8780 (−7)
	3.00 (5) to 5.00 (5)	1	9.7667 (−15)	2.0137 (−6)
	5.00 (5) to 1.00 (6)	0	2.6000 (− 9)	5.5385 (−6)
N III	7.80 (4) to 1.05 (5)	7	1.6085 (−47)	3.2556 (−5)
	1.05 (5) to 1.65 (5)	5	7.2377 (−37)	7.8635 (−7)
	1.65 (5) to 2.22 (5)	3	7.3287 (−27)	1.2349 (−5)
	2.22 (5) to 3.40 (5)	2	1.2646 (−21)	1.7178 (−5)
	3.40 (5) to 5.00 (5)	1	2.6618 (−16)	2.9558 (−5)
	5.00 (5) to 1.00 (6)	1	3.9000 (−15)	1.5385 (−7)
N IV	1.40 (5) to 2.00 (5)	6	7.8118 (−44)	5.0009 (−6)
	2.00 (5) to 3.40 (5)	4	4.4884 (−33)	1.9625 (−6)
	3.40 (5) to 6.00 (5)	2	5.4328 (−22)	1.7420 (−6)
	6.00 (5) to 1.00 (6)	1	2.8667 (−16)	2.2093 (−6)
N V	2.00 (5) to 3.10 (5)	5	2.4560 (−39)	1.3619 (−6)
	3.10 (5) to 5.00 (5)	4	1.0482 (−33)	1.0638 (−7)
	5.00 (5) to 8.00 (5)	1	1.3833 (−17)	1.7952 (−5)
	8.00 (5) to 1.00 (6)	1	1.5060 (−16)	5.1383 (−7)

*Indicates power of ten by which significant figures are multiplied.

TABLE 2 (cont)

Ion	Temperature Range	n	G	H
O I	1.95 (4) to 2.55 (4)	8	2.1502 (−47)	6.2801 (−5)
	2.55 (4) to 3.60 (4)	6	1.3135 (−38)	6.9377 (−5)
	3.60 (4) to 6.20 (4)	4	4.8269 (−29)	6.4848 (−6)
	6.20 (4) to 1.00 (5)	2	3.1962 (−20)	1.1515 (−4)
	1.00 (5) to 2.00 (5)	2	4.0000 (−19)	0.
	2.00 (5) to 4.00 (5)	1	6.7500 (−14)	9.2593 (−7)
	4.00 (5) to 1.00 (6)	0	1.8333 (− 8)	2.5455 (−6)
O II	5.80 (4) to 8.00 (4)	7	3.8980 (−46)	2.7911 (−6)
	8.00 (4) to 1.25 (5)	5	2.6517 (−36)	1.8859 (−6)
	1.25 (5) to 2.00 (5)	3	2.4033 (−26)	9.0430 (−6)
	2.00 (5) to 3.50 (5)	2	9.7313 (−21)	1.9364 (−6)
	3.50 (5) to 6.60 (5)	1	3.6125 (−15)	1.6622 (−6)
	6.60 (5) to 1.00 (6)	0	1.1176 (− 9)	5.2632 (−6)
O III	9.80 (4) to 1.40 (5)	6	6.6399 (−43)	7.1442 (−6)
	1.40 (5) to 2.30 (5)	4	1.0936 (−32)	9.8591 (−6)
	2.30 (5) to 5.00 (5)	2	9.1104 (−22)	4.6737 (−6)
	5.00 (5) to 1.00 (6)	1	1.0400 (−15)	9.2308 (−7)
O IV	1.50 (5) to 2.20 (5)	6	8.6918 (−44)	6.6986 (−8)
	2.20 (5) to 4.00 (5)	3	1.7726 (−28)	1.9536 (−5)
	4.00 (5) to 1.00 (6)	1	1.6667 (−17)	3.5000 (−5)
O V	2.50 (5) to 3.90 (5)	5	8.7337 (−40)	6.8985 (−7)
	3.90 (5) to 6.60 (5)	3	1.1063 (−28)	1.3431 (−6)
	6.60 (5) to 1.00 (6)	2	1.3336 (−22)	4.9821 (−8)
O VI	3.50 (5) to 6.00 (5)	4	5.1901 (−35)	8.1078 (−7)
	6.00 (5) to 1.00 (6)	2	1.3944 (−23)	1.6534 (−6)

THREE-BODY RECOMBINATION

Definition of the Process

Consider the physical situation in which two free electrons simultaneously pass within a small distance of a positive ion. As a result of the Coulomb interaction between the three particles, it is possible for one electron to lose sufficient energy to settle into a bound quantum state while the second electron remains free and moves in such a way that energy and momentum are conserved. Symbolically, this process can be represented by

$$X^+ + 2e \rightarrow X^* + e^-.$$
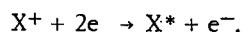
In this expression, X^* denotes an atom in either the ground state or one of the quantized excited states. It should be noted that this process is the inverse of the electron-impact ionization reaction. This fact will be used in determining the recombination rate.

It can be seen that recombination processes are inherently more difficult to analyze than ionization processes because of the greater number of "channels" through which the reaction can occur. In fact, three-body recombination yielding excited bound states occurs at a considerably higher rate than does recombination yielding the ground state.

Derivation of the Recombination Rate Expression

The simplest method for finding the rate at which various bound states are formed by recombination is to use the principle of detailed balance. The essence of this principle can be stated as follows: In the case of thermodynamic equilibrium, the number of particles leaving a given quantum state via some process is equal to the number of particles entering this state via the inverse process (Ref 8). Because of this principle, it is possible to equate the rates for the direct and inverse reactions to get

$$n_e^2 \, n_i \, \beta_m = n_e \, n_m \, \alpha_m \tag{12}$$

In this expression n_m is the density of atoms in the state having principal quantum number m, and n_i and n_e are the densities of ions and free electrons, respectively. In addition, α_m is the electron-impact ionization rate

13

coefficient for removal of an electron from an atom in state m, and β_m is the three-body recombination rate coefficient for the formation of an atom in state m. By combining the Saha and Boltzmann formulas (Ref 9, pp 36, 37), we obtain

$$\frac{n_e \, n_i}{n_m} = \phi \, (m, \, T) = \frac{g_{r \, + \, 1, \, 1}}{g_{r, \, m}} \, \frac{2(2\pi \, m_e \, kT)^{3/2}}{h^3} \, e^{-\frac{I_m}{kT}}$$

so that

$$\beta_m = \frac{g_{r, \, m}}{g_{r \, + \, 1, \, 1}} \, \frac{h^3}{2(2\pi \, m_e \, kT)^{3/2}} \, \alpha_m \tag{13}$$

where I_m is the ionization potential of the mth bound state, m_e is the electron mass, $g_{r, \, m}$ and $g_{r \, + \, 1, \, 1}$ are the statistical weights of the mth bound state of an r-times ionized atom and the ground state of an (r + 1)-times ionized atom, respectively, and h is Planck's constant. By using Equation 13, it is possible to calculate the rate coefficients β_m when the rate coefficients for the inverse reactions are known.

Radiative Decay of Excited States

In most situations where nonequilibrium conditions exist, a number more useful than the rate at which atoms are formed in various excited states is the rate at which ground state atoms are formed either directly or by radiative decay of atoms formed in excited states. Indeed, the formation of a ground state atom is the definition of a recombination event which D'Angelo (Ref 10) used in his calculation of three-body recombination rates in hydrogen. This definition is used for the rate calculations described here.

Consider an electron which is captured during the formation of an excited ionic state. Two processes can occur: (a) the electron spontaneously undergoes a radiative transition to a lower quantum level, or (b) the electron is re-ionized by a collision with a free electron before de-excitation can occur. Thus, the ultimate number of ground state atoms depends upon the relative probability of making the next radiative transition at each step of the cascade process.

14

The assumption that an electron in an excited state has only two alternatives for relaxation neglects collisional excitation and de-excitation transitions between excited states. The omission of these reactions is probably justified because, as D'Angelo points out, collisional transitions occur mainly to neighboring states, so excitation and de-excitation processes will tend to compensate. In addition, Giovanelli (Ref 11) has found that, at least in hydrogen plasmas, the rates of collisional transition usually do not exceed the rates of collisional ionization.

Specialization to the Formation of Hydrogenic Ions

Because of the large number of channels through which recombination can occur, theoretical treatment of the recombination process for arbitrary ions is not feasible. Rather than attempt this task, calculations have been performed to determine the rate of three-body recombination of completely stripped nitrogen and oxygen nuclei to form hydrogenic ions. With this specialization, Equation 13 can be simplified by using the fact that the statistical weights of the bare nucleus and the one-electron ion in state m are 1 and $2m^2$, respectively. Thus Equation 13 becomes

$$\beta_m = \frac{h^3 \, m^2}{(2\pi \, m_e \, kT)^{3/2}} \, e^{\frac{I_m}{kT}} \, \alpha_m \qquad (14)$$

Only electric dipole transitions need to be considered for the radiative decay of the excited ions. Hence, use of the well-known selection rule $\Delta \ell = \pm 1$ permits a systematic enumeration of all allowed transitions for an arbitrary maximum value of the principal quantum number. For the one-electron ions formed by the process considered here, quantum mechanical results for the radiative transition probabilities are given by Bethe and Salpeter (Ref 12). By a slight generalization of formulas given by these authors, the dipole transition probabilities for hydrogenic ions are found to be

$$P_{m\,\ell}^{m'\,\ell-1} = \frac{8.0}{3} \times 10^9 \left(\frac{\ell}{2\ell+1}\right) \frac{Z^4 \, (m+m')^3 \, (m-m')^3}{m^6 \, m'^6} \left[\frac{R_{m\,\ell}^{m'\,\ell-1}}{a_Z}\right]^2 \quad \text{sec}^{-1} \qquad (15a)$$

and

$$P_{m\,\ell}^{m'\,\ell+1} = \frac{8.0}{3} \times 10^9 \left(\frac{\ell+1}{2\ell+1}\right) \frac{Z^4 \, (m+m')^3 \, (m-m')^3}{m^6 \, m'^6} \left[\frac{R_{m'\,\ell+1}^{m\,\ell}}{a_Z}\right] \quad \text{sec}^{-1} \qquad (15b)$$

15

where m and ℓ are the principal and orbital quantum numbers, respectively, of the initial state and m' is the principal quantum number of the final state, $R^{m'\,\ell-1}_{m\,\ell}$ is the integral

$$R^{m'\,\ell-1}_{m\,\ell} = \int_0^\infty R_{m\,\ell} R_{m'\,\ell-1}\ r^3\,dr = R^{m\,\ell}_{m'\,\ell-1}$$

involving radial wavefunctions, and a_Z is the "Bohr radius" for the hydrogenic ion with atomic number Z. A general expression for $R^{m'\,\ell-1}_{m\,\ell}$ quoted by Bethe and Salpeter, is

$$\frac{R^{m'\ell-1}_{m\ell}}{a_Z} = \frac{(-1)^{m'-\ell}}{4\,(2\ell-1)!}\left[\frac{(m+\ell)!\,(m'+\ell-1)!}{(m-\ell-1)!\,(m'-\ell)!}\right]^{1/2}\ \frac{4\,(mm')^{\ell+1}\,(m-m')^{m+m'-2\ell-2}}{(m+m')^{m+m'}}\ \times$$

$$\left\{F\left(-m_r,\,-m'_r,\,2\ell,\,-\frac{4mm'}{(m-m')^2}\right)-\left[\frac{m-m'}{m+m'}\right]^2\,F\left(-m_r-2,\,-m'_r,\,2\ell,\,-\frac{4mm'}{(m-m')^2}\right)\right\}$$

In this expression, $F(\alpha,\,\beta,\,\gamma,\,X)$ is the hypergeometric function and $m_r = m-\ell-1$, $m'_r = m'-\ell$ are the radial quantum numbers of the two states.

The Recombination Rate

In order to describe the procedure by which the recombination rate was calculated, consider Figure 6 (p 29), which shows all possible states in which hypothetical hydrogenic ions with four quantum levels can exist. It is assumed that the number of ions in any particular state is being increased at a rate given by Equation 12 and that the ions formed in state m are distributed over the ℓ sublevels according to the statistical weight factor $(2\ell+1)/m^2$.

Two approaches for considering the redistribution of excited-state ions are possible. The first of these is to start with a given number of ions existing with certain (m,ℓ) and then keep track of the number of ions which radiate at each step of the cascade. Let $P(m,\ell \to m',\ell')$ be the relative probability that an electron undergoes a radiative transition between the indicated states. If, for example, $N(4,3)$ is the number of atoms with quantum

16

numbers $(4,3)$, then the number of such atoms finally decaying to the ground state is

$$N(4,3) \times P(4,3 \to 3,2) \times P(3,2 \to 2,1) \times P(2,1 \to 1,0).$$

The second approach is to determine the redistribution of all ions originally in the highest quantum state after one radiative transition from this level. The number of these particles going to particular lower levels is then added to the original concentrations and the procedure is repeated at the next lower level. Thus, for example, the concentration with $(3,2)$ is changed from its original value of $N(3,2)$ to

$$N(3,2) + N(4,3) P(4,3 \to 3,2) + N(4,1) P(4,1 \to 3,2).$$

Similarly, the concentrations for all levels below $m = 4$ are augmented by the ions originally having $m = 4$ which radiated before experiencing electron-impact ionization. The final result for the number of atoms decaying to the ground state is obviously the same using either approach. The results to be presented later were calculated using the second approach.

Now consider the calculation of the relative transition probabilities. Formally, the constant in the spontaneous transition rate expression

$$\frac{d n_{m,\ell}}{dt} = - P_{m\ell}^{m',\ell'} \ n_{m,\ell}$$

is obtained from either Equation 15a or 15b. It has been shown that the electron-impact ionization rate is given by

$$\frac{d n_{m,\ell}}{dt} = - \alpha_m n_e \ n_{m,\ell}$$

Thus it can be seen that the quantity $\alpha_m n_e$ gives the transition probability for electron-impact ionization. Then, for example, to calculate the relative probability for the radiative transition $(3,1) \to (1,0)$, it is necessary to evaluate

$$P(3,1 \to 1,0) = \frac{P_{3,1}^{1,0}}{\alpha_3 n_e + P_{3,1}^{1,0} + P_{3,1}^{2,0}}$$

17

using Equation 15a and the values for a_3 calculated in the manner described in the electron-impact ionization section.

The Rate Coefficient Calculation

An effective recombination rate coefficient can be obtained by dividing the rate at which ground-state ions are formed by $n_e^2 n_i$. A computer program has been written for the IBM 709 to calculate this rate coefficient. The program calculates the initial distribution of recombined states, the radiative transition probabilities, the re-ionization rates, the relative probabilities for radiative decay, and the successive distributions of recombined states which lead to the final number of ions reaching the ground state.

Calculations were performed with the assumption that $m = 10$ is the highest populated level. Although higher states are actually populated and the rate of population increases with the value of m, their contribution to the ground state population rate is small for two reasons. First, the re-ionization rate also increases with m, so the relative probability of radiative de-excitation becomes small. And second, the levels (m, 1) which can populate the ground state with a single efficient transition are not populated strongly because of the statistical factor $(2\ell + 1)/m^2$.

The presence of free charges in the vicinity of the hydrogenic ions lowers the position of the ionization continuum of the latter and causes only a finite number of bound ionic states to exist. Estimates of the effects due to the presence of free charges have been made using the results of Griem (Ref 13). These calculations indicate that only for the highest electron concentration considered here could this free-charge effect have any appreciable influence on the present calculations. Thus, for the sake of simplicity, neither this effect nor the concurrent shift in position of the bound ionic states has been considered here.

At the highest temperatures considered in these calculations, there is a question as to whether the ground state is populated appreciably under equilibrium conditions because of collisional effects. However, by using the Boltzmann factor, the population ratio n_2/n_1 is found to be less than 10^{-3} for all situations considered here. Hence, it seems reasonable to assume that the cascade process does actually proceed all the way to the ground state.

18

The results for the effective rate constants for oxygen and nitrogen nuclei forming hydrogenic ions are shown in Figures 7 and 8 (pp 30 and 31). These results can be approximated analytically by an expression of the form

$$\beta (T, n_e) = m(n_e) T^{r(n_e)}$$

Values for $m(n_e)$ and $r(n_e)$ were found by first assuming that β varied as some inverse power of the temperature for constant electron concentration. Then, using the values for $m(10^{15})...m(10^{18})$, $r(10^{15})...r(10^{18})$, the $m(n_e)$ and $r(n_e)$ were fit to polynomials in $\log n_e$ by a least squares analysis. The results were found to be:

For nitrogen

$$m(n_e) = (-5.329 + 0.4166 \log n_e) \times 10^{-20}$$

$$r(n_e) = [-3.41715 + 0.30504 \log n_e - 0.01195 (\log n_e)^2]$$

For oxygen

$$m(n_e) = [80.887 - 10.753 \log n_e + 0.3585 (\log n_e)^2] \times 10^{-20}$$

$$r(n_e) = [-4.08684 + 0.42122 \log n_e - 0.01641 (\log n_e)^2]$$

These expressions are valid in the temperature range $8 \times 10^4 \leq T \leq 10^6$ °K and give results which are generally within 20% of the values found with the computer.

RADIATIVE RECOMBINATION

Definition of the Process

Consider the physical situation in which a free electron passes very near a charged ion. Because of the interaction between the charges of the electron and the ion, it is possible for the electron to become bound to the ion, with the excess energy of the system being radiated away as an electromagnetic photon. This process can be represented symbolically by

$$X^+ + e^- \to X + \gamma$$

19
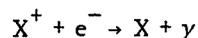
where γ represents the photon. This process is known as radiative recombination.

Derivation of the Recombination Rate Constant

Because of the complexity of treating recombination involving arbitrary ions, only the recombination of bare nuclei with free electrons to form hydrogenic ions will be considered here. The rate for the radiative recombination process can be determined most easily by using cross section information for the inverse reaction and the principle of detailed balance. Using the result quoted by Richards (Ref 14) for the relation between the photoionization and radiative recombination cross sections, it is possible to write

$$\sigma^{(m)}_{rec} = \left(\frac{h\nu}{c\, m_e v}\right)^2 \frac{g_m}{g_B}\, \sigma^{(m)}_{ion} \tag{16}$$

where $h\nu = I_m + \frac{1}{2} m_e v^2$ expresses the conservation of energy, and g_B and g_m are, respectively, the statistical weights of the bare nucleus and the ion in state m.

Since recombination leading to excited states is not negligible, a realistic calculation of the rate requires that this fact be considered. An approximate expression for the photoionization cross section of hydrogenic ions as a function of the principal quantum number is quoted by Ambartsumyan (Ref 9, p 42). This expression is

$$\sigma^{(m)}_{ion} = \frac{64\, \pi^4\, \epsilon^{10}\, m_e\, Z^4\, g'}{3\, \sqrt{3}\, c\, h^6\, \nu^3\, m^5} \tag{17}$$

where g' is a correction factor little different from unity and the other symbols have their usual meanings. Now the statistical weights for the initial and final states are, respectively, 1 and $2 m^2$. From Equations 16 and 17, and the definitions

$$I_m = \frac{Z^2\, \epsilon^4\, m_e}{2 h^2\, m^2}$$

20

and for ionization potential and

$$\phi_o = \frac{8\pi}{3} \frac{\epsilon^4}{(m_e c^2)^2} = 0.6652 \times 10^{-24} \text{ cm}^2$$

for the Thomson cross section, it follows that

$$\sigma_{rec}^{(m)} = \frac{2}{\sqrt{3}} \frac{Z^2 m_e c^2 \alpha \phi_o}{m} \frac{I_m}{E_e (I_m + E_e)} \tag{18}$$

where $\alpha = \epsilon^2/\hbar c$ is the fine-structure constant.

If it is assumed that the energy distribution of the free electrons is Maxwellian, then the recombination rate for the formation of hydrogenic ions in state m is given by

$$\text{Rate} = \int_o^\infty n_e n_B f(E_e) \sigma_{rec}^{(m)} (E_e) \left(\frac{2 E_e}{m_e}\right)^{\frac{1}{2}} d E_e \tag{19}$$

where $f(E_e) dE_e$ is the normalized Maxwellian distribution function and n_B is the concentration of bare nuclei. When the recombination rate is written in the form

$$\frac{dn_e}{dt} = -K_m n_B n_e,$$

use of Equation 19, with the appropriate substitutions, shows that the rate coefficient K_m is given by

$$K_m = \left(\frac{m_e c^2}{3\pi}\right)^{\frac{1}{2}} \left(\frac{2}{kT}\right)^{\frac{3}{2}} \frac{(2Z \alpha \phi_o c I_1)}{m^3} \exp (I_1/m^2 kT) [-Ei (-I_1/m^2 kT)]. \tag{20}$$

Radiative Deexcitation of Recombination States

As in the case of three-body recombination, it is desired to know the rate at which ground-state ions are formed. As before, formation is assumed to occur either directly or by radiative decay of excited states. Since the radiative deexcitation process is independent of the mechanism by which

21

an excited ion is formed, all the discussion concerning the decay cascade given in the section on three-body recombination applies here as well.

The Rate Coefficient Calculation

A computer program for the IBM 709 was written to compute the rate coefficient for the formation of hydrogenic ions in the ground state. This program calculates the initial population of the excited states using Equation 20 and the successive distributions of recombined states. Figure 9 (p 32) shows the results of calculations performed for bare oxygen and nitrogen nuclei, respectively.

For radiative recombination, in contrast to three-body recombination, the rate at which excited states are formed falls off with increasing m. Hence, the contribution to the ground-state recombination due to states above $m = 10$ is quite insignificant. A consequence of the fact that the main contribution to the ground-state recombination comes from low-lying states is that the effect of electron impact reionization is quite small. Therefore, the dependence of the rate coefficient on the free electron density is slight. In fact, the calculations show that the rate coefficient is essentially independent of the electron density.

To utilize these recombination data in computer calculations, analytical approximations for the curves shown in Figure 9 were obtained. The desired expressions were found to be:

For nitrogen

$$K = (7.761 \times 10^{-9}) \, T^{-0.60360}; \; 3 \times 10^{4} \leq T < 2 \times 10^{5} \; {}^{\circ}K$$

$$K = (1.721 \times 10^{-8}) \, T^{-0.66881}; \; 2 \times 10^{5} \leq T \leq 10^{6} \; {}^{\circ}K$$

For oxygen,

$$K = (8.054 \times 10^{-9}) \, T^{-0.58040}; \; 3 \times 10^{4} \leq T < 2 \times 10^{5} \; {}^{\circ}K$$

$$K = (1.952 \times 10^{-8}) \, T^{-0.65294}; \; 2 \times 10^{5} \leq T \leq 10^{6} \; {}^{\circ}K$$

Values obtained with these approximate expressions are within 5% of the computer results.

22

REFERENCES

1. M. Gryziński, *Phys. Rev. 115*, 374 (1959)

2. C. Moore, *Atomic Energy Levels As Derived From the Analyses of Optical Spectra*, Vol. 1, National Bureau of Standards Circular 467, U. S. Government Printing Office, 1948

3. J. C. Slater, *Quantum Theory of Matter*, McGraw-Hill, New York, 1951, p 476

4. E. Trefftz, *Proc. Roy. Soc. (A) 271*, 379 (1963)

5. W. L. Fite and R. T. Brackmann, *Phys. Rev. 113*, 815 (1959)

6. M. J. Seaton, *Phys. Rev. 113*, 814 (1959)

7. L. Spitzer, *Physics of Fully Ionized Gases*, Interscience Pub. Co., New York, 1956

8. G. S. Ivanov-Kholodnyi, G. M. Nikol skii, and R. A. Gulyaev, *Astronomicheskii Zhurnal 37*, 799 (1960): Translation Soviet Astronomy AJ 4, 754 (1961)

9. V. A. Ambartsumyan, *Theoretical Astrophysics*, Pergamon, New York, 1958, pp 36, 37, 42

10. N. D'Angelo, *Phys. Rev. 121*, 505 (1961)

11. R. G. Giovanelli, *Australian J. Sci. Research A1*, 275 (1948)

12. H. A. Bethe and E. E. Salpeter, *Quantum Mechanics of One- and Two-Electron Atoms*, Academic Press, New York, 1957

13. H. A. Griem, *Phys. Rev. 128*, 997 (1962)

14. P. I. Richards, *Manual of Mathematical Physics*, Pergamon, New York, 1959, p 149

23

Semiclassical Theory $E_1 = 127$ ev, $U = 13.6$ ev

• = experimental points given by Fite and Brackmann

Curve with $E_1 = 100$ ev

Curve with $E_1 = 150$ ev

$\frac{\sigma_i}{\pi a_o^2}\left(\frac{1}{3.7}\right)$

$\sigma_i/\pi a_o^2$

E_1 (ev)
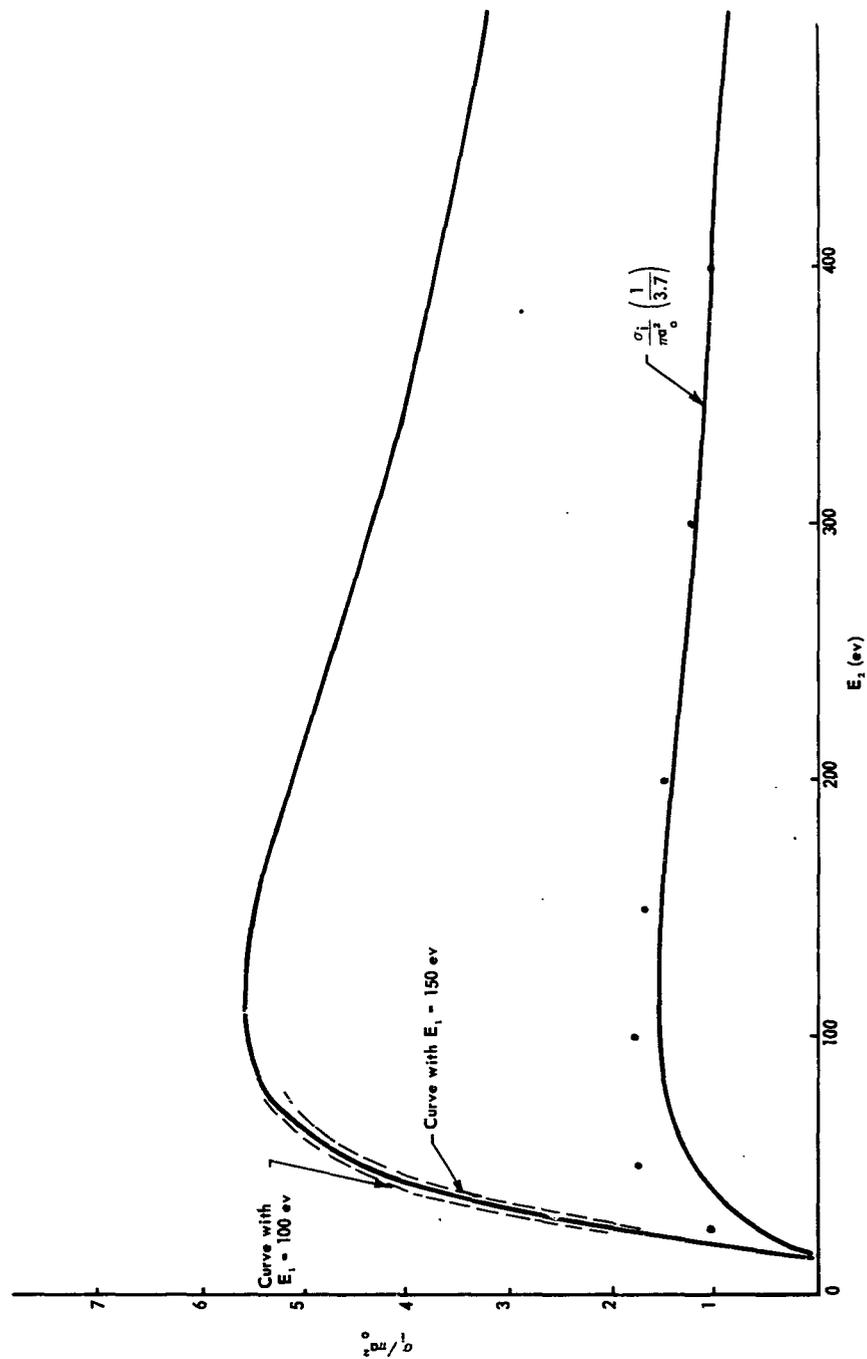
Fig 1   Electron impact ionization cross section for O

24

Semiclassical Theory $E_1 = 89.0$ ev, $U = 14.5$ ev
x = Points from Seaton

$$\sqrt{\frac{\sigma_i}{\pi a_o^2}} \left(\frac{1}{1.683} \right)$$

E_1 (ev)

$\sigma_i / \pi a_o^2$
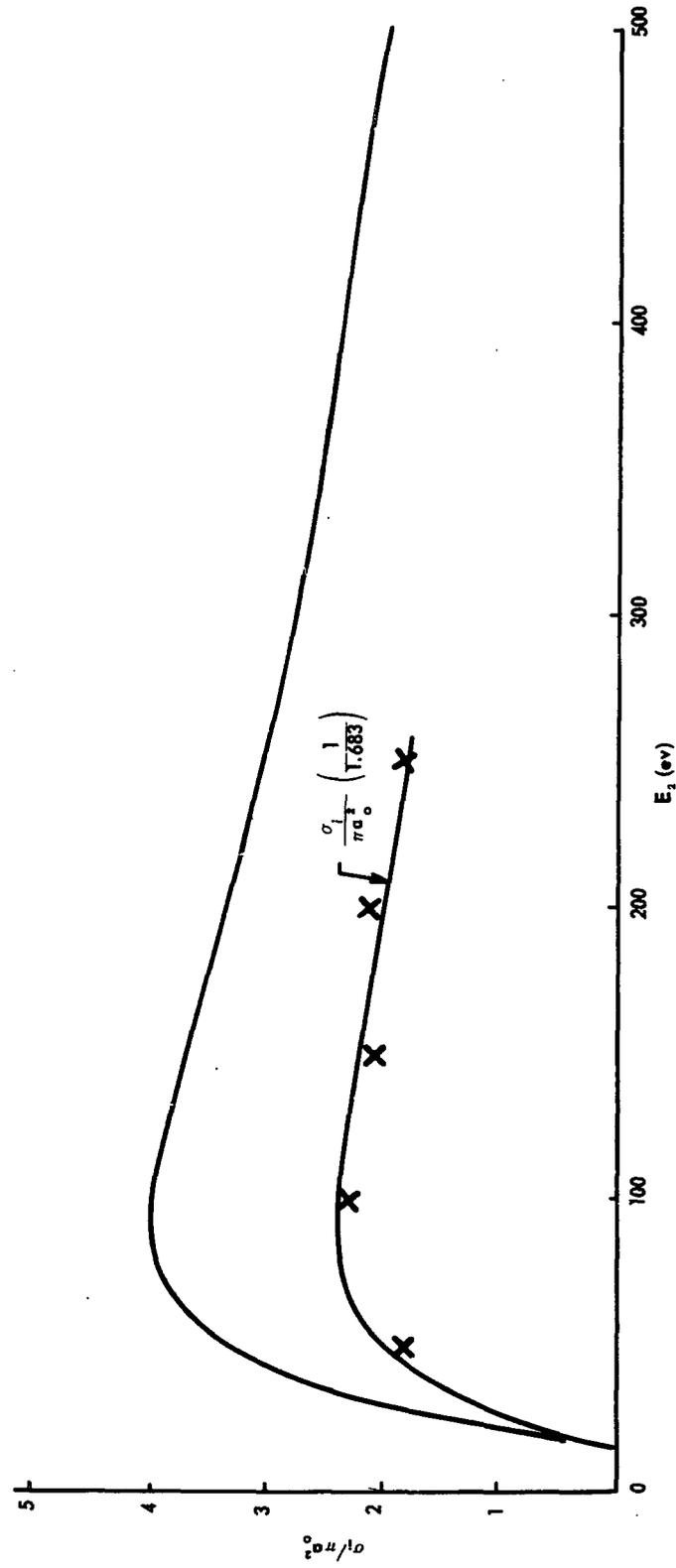
Fig 2   Electron impact ionization cross section for N

25
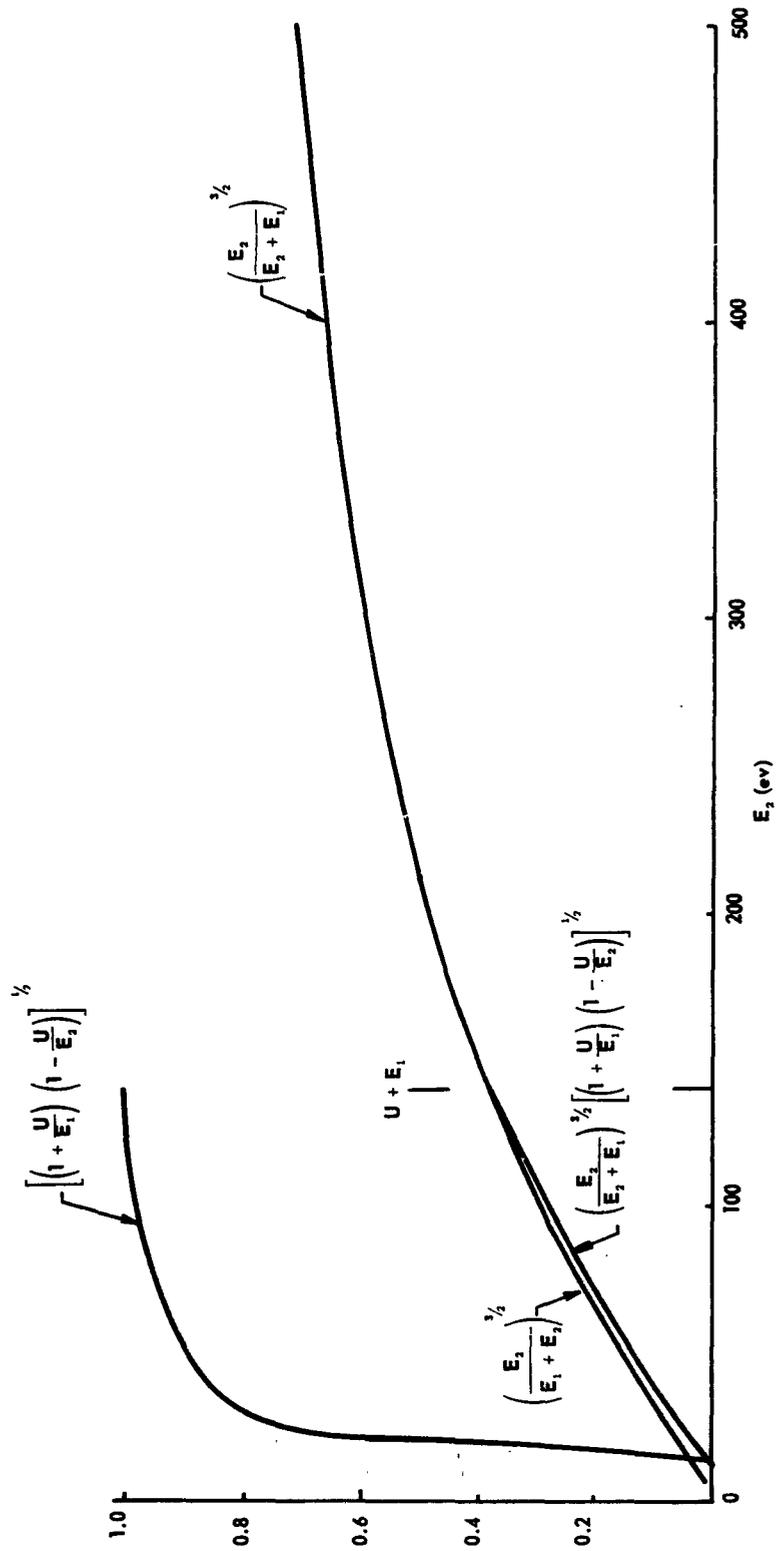
Fig 3   Energy dependence of certain factors governing the ionization rate for oxygen   (U = 13.6 ev, E_1 = 127)

26
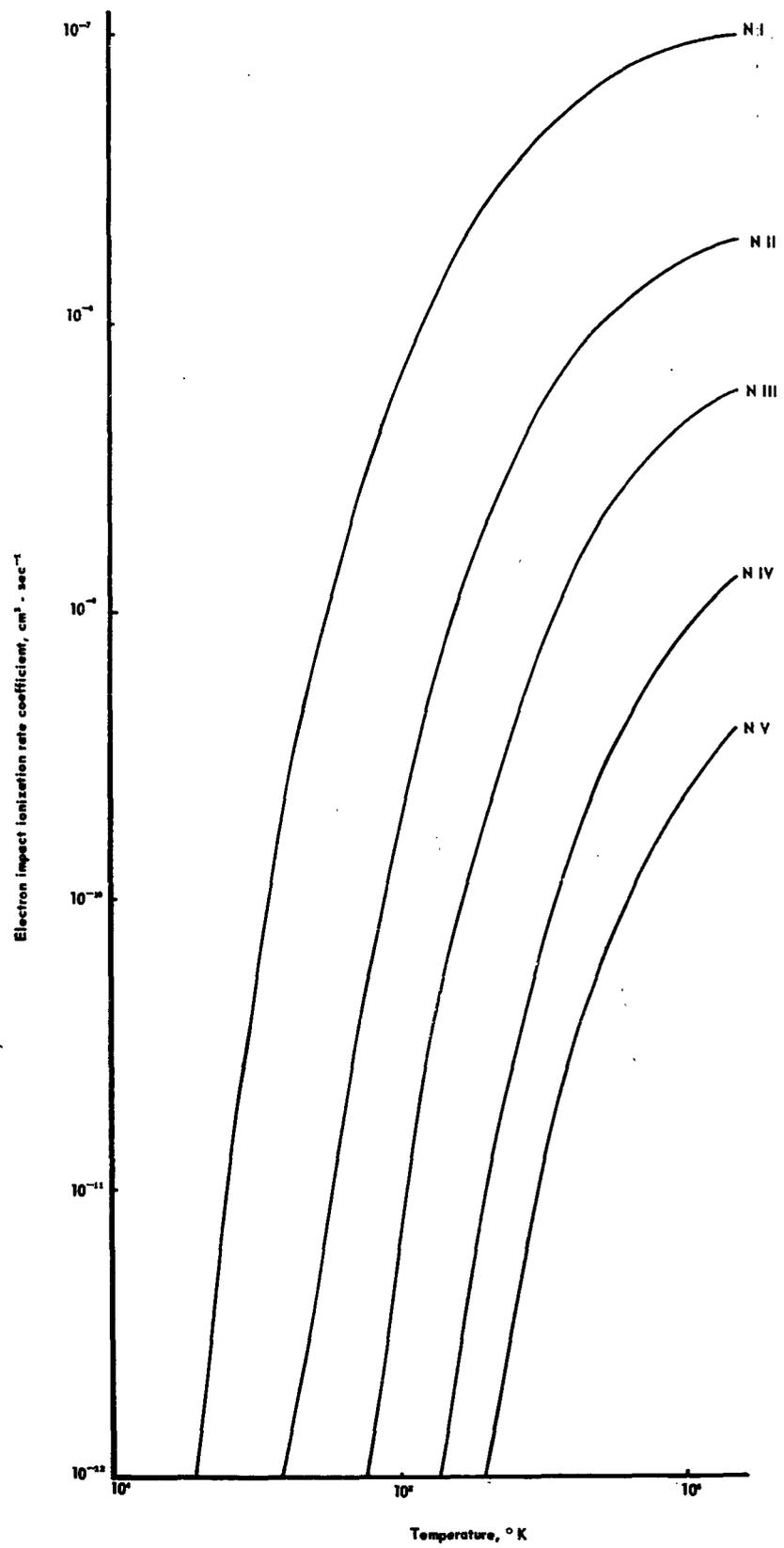
Fig 4   Ionization rate coefficient for electrons incident on nitrogen ions

27
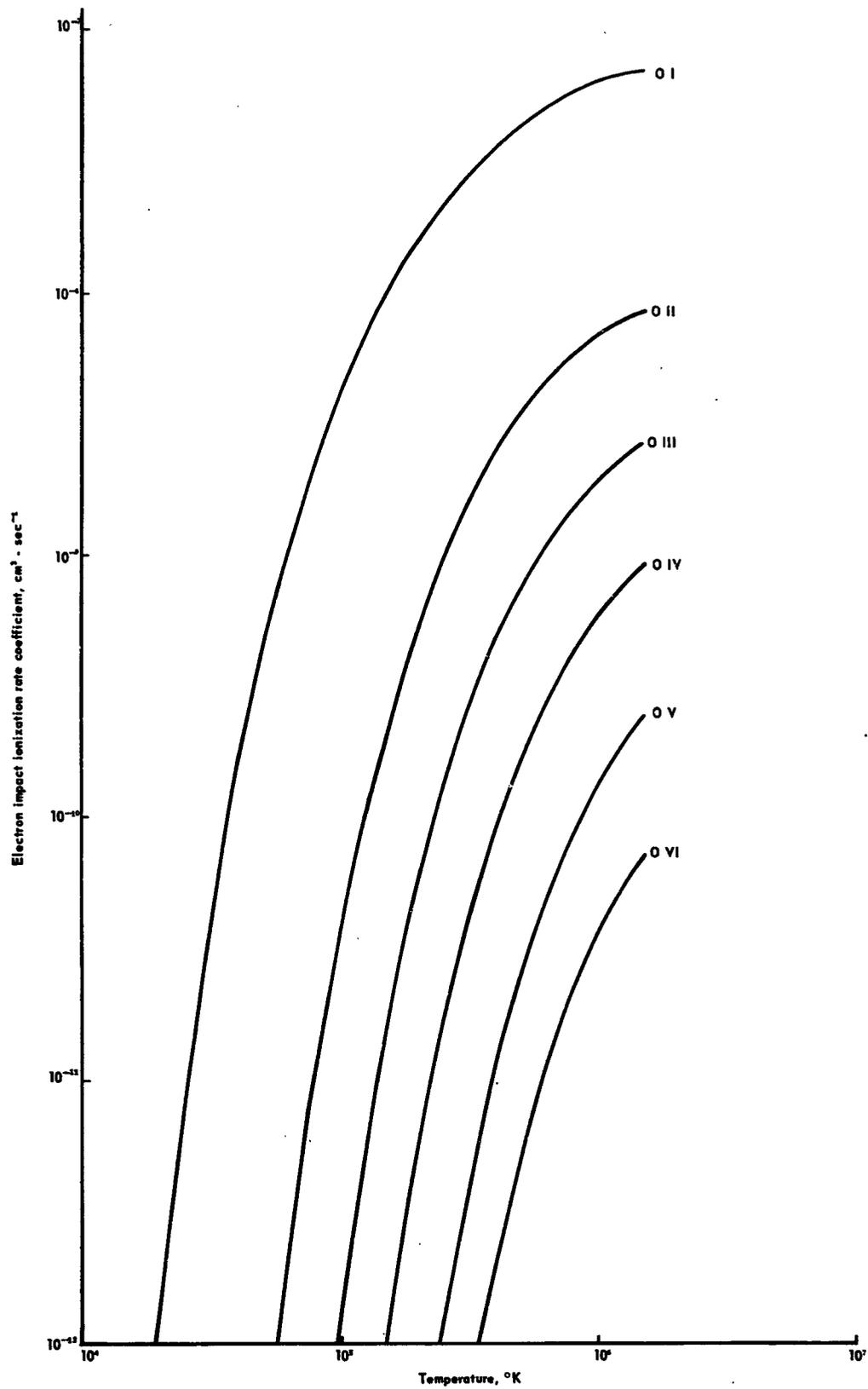
Fig 5   Ionization rate coefficient for electrons incident on oxygen ions

28
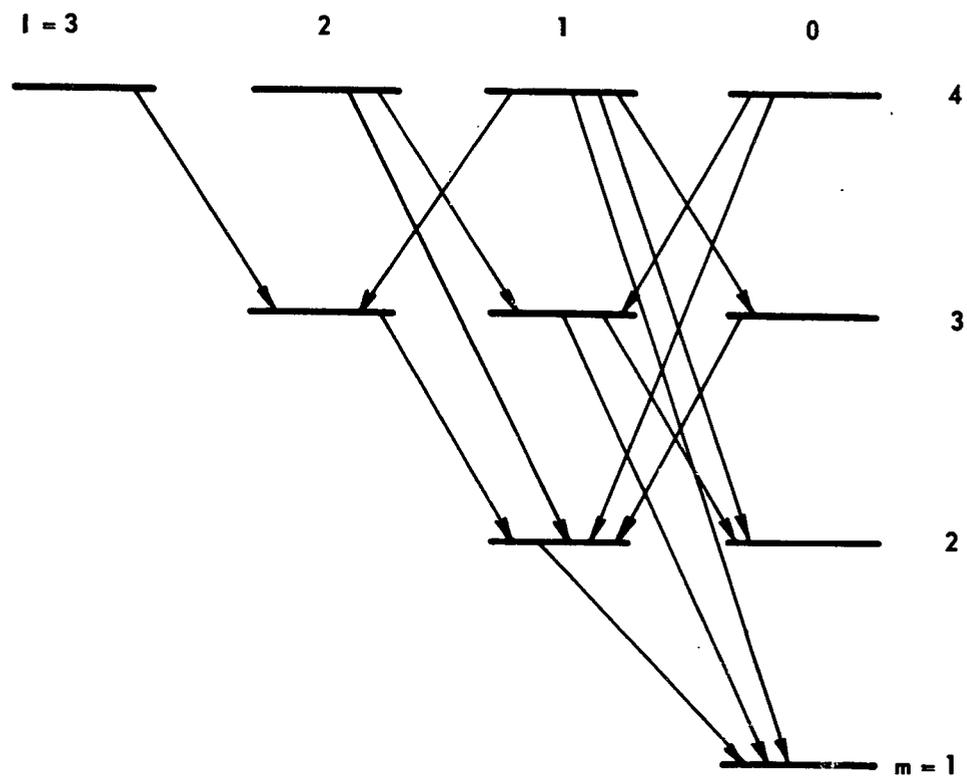
Fig 6   Possible radiative transitions for hypothetical four-level atom
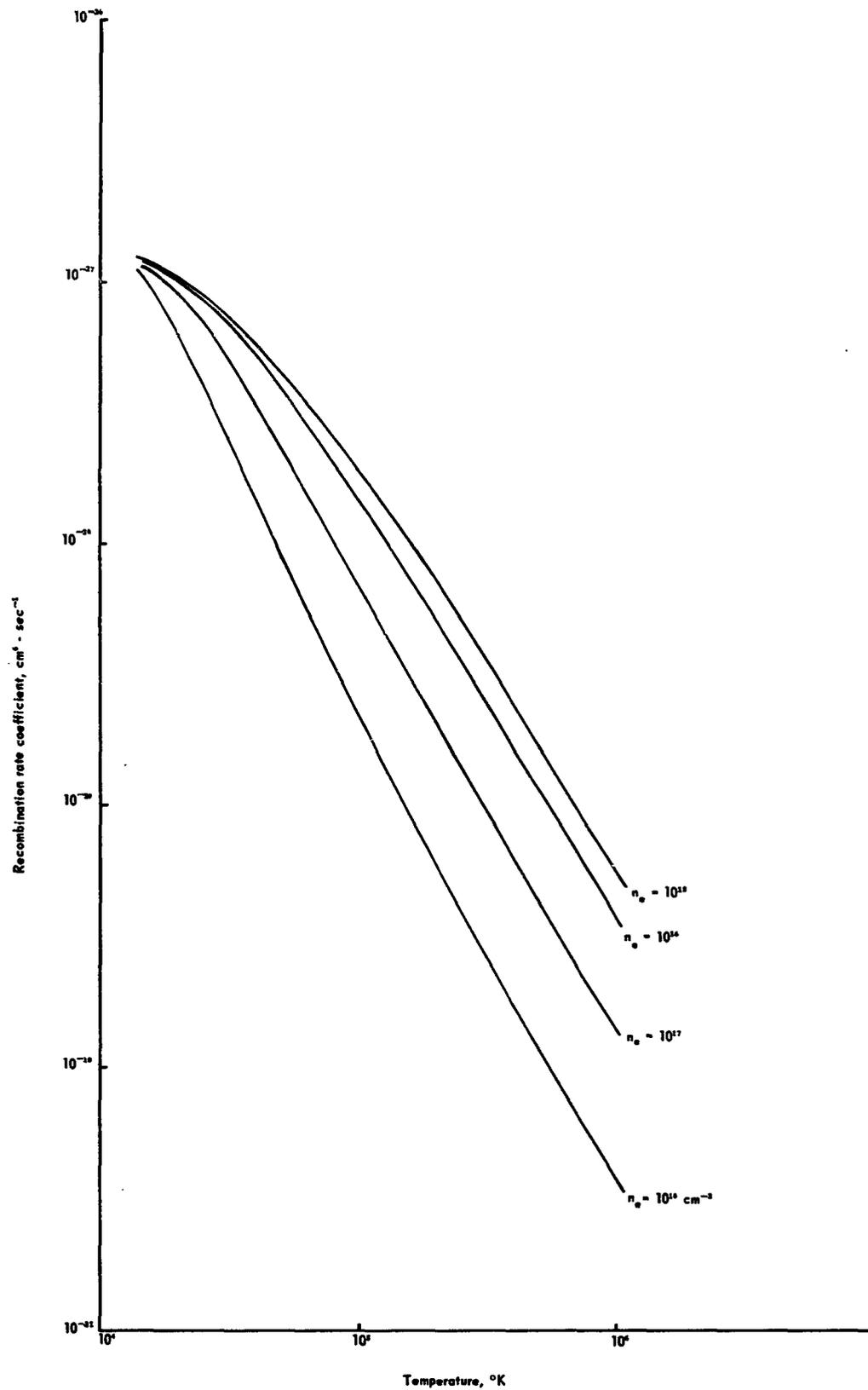
Fig 7   Three-body recombination rate coefficient for the formation of N^{6+} ions in the ground state
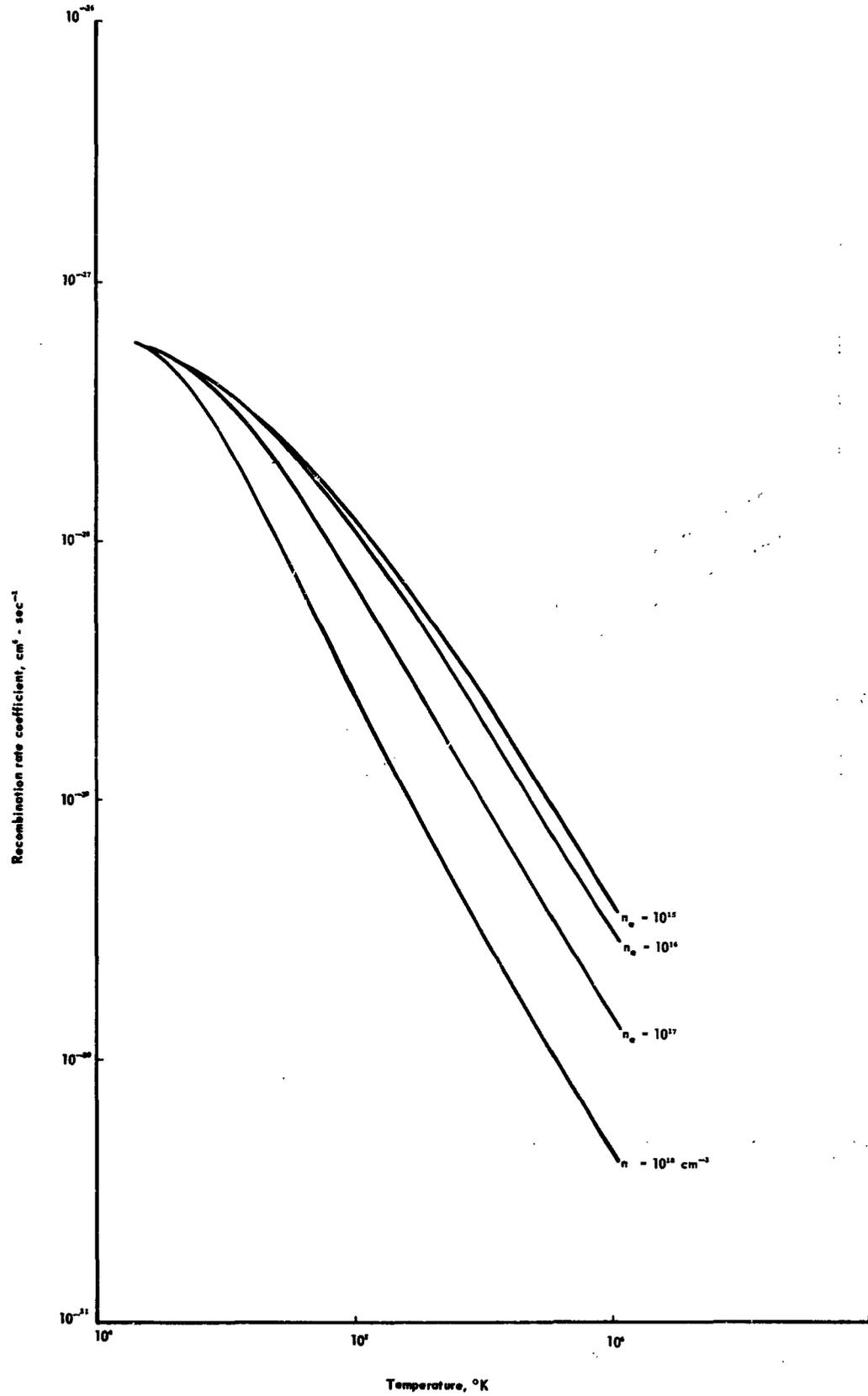
Fig 8   Three-body recombination rate coefficient for the formation of O^{7+} ions in the ground state

31
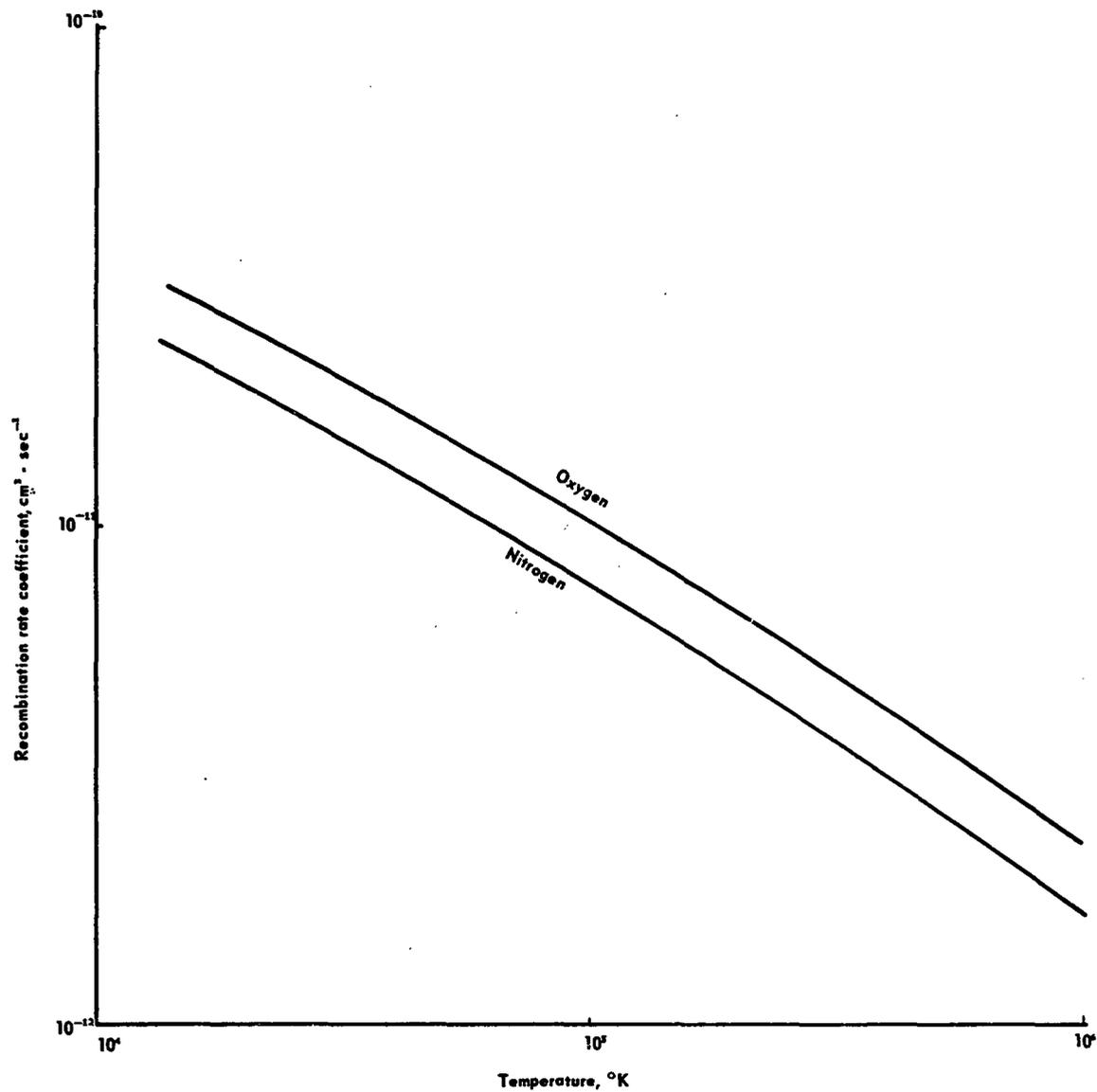
Fig 9   Radiative recombination rate coefficients for the formation of N^{6+} and O^{7+} ions in the ground state

32

DISTRIBUTION LIST

Commanding Officer
Harry Diamond Laboratories
ATTN: Technical Reference Center   17 - 18
Washington 25, D. C.

Commanding Officer
Ballistic Research Laboratories
ATTN: E. Minor   19
        J. Meszaros   20
        E. Baicy   21
        O. Johnson   22
Aberdeen Proving Ground
Maryland

Commanding General
White Sands Missile Range
ATTN: Technical Library   23
New Mexico

Commander
Headquarters, CONAD
Ent Air Force Base
Colorado Springs, Colorado   24

Director
U. S. A. Combat Development Command
Nuclear Group
ATTN: ATSWB   25
Ft. Bliss, Texas

Commanding Officer
U. S. A. Combat Development Command
Air Defense Agency
ATTN: Mr. Sisco   26
Ft. Bliss, Texas

President
U. S. Army Air Defense Board
ATTN: ATBD   27
Ft. Bliss, Texas

Commanding General
U. S. Continental Army Command
ATTN: ATDEV   28
Ft. Monroe
Virginia

Commander
Headquarters, ARADCOM
Ent Air Force Base
ATTN: Maj. P. Farrell   29
Colorado Springs, Colorado

Chief
Headquarters
Defense Atomic Support Agency
ATTN: Col. S. E. Singer   30
            Maj. L. Logie   31
            Mr. J. Kelso   32
            Technical Library   33
Washington 25, D. C.

Commander
Defense Atomic Support Agency
ATTN: Nuclear Branch   34
            Vulnerability Branch   35
            Technical Library   36
Sandia Base
Albuquerque, New Mexico

Defense Documentation Center
Cameron Station
Alexandria, Virginia   37 - 56

Director
Advanced Research Projects Agency
ATTN: Maj. C. Sherwood   57
            Dr. D. Fitz   58
            Technical Library   59
Washington 25, D. C.

35

Chief
Bureau of Naval Weapons
ATTN: SP-2721   60
Navy Dept.
Special Project Office
Washington 25, D. C.

Commander
Naval Ordnance Laboratories
ATTN: J. Noulton   61
        L. Rudlin   62
Silver Spring 19, Maryland

Director
U. S. Naval Research Laboratory
ATTN: Technical Library   63
Washington 25, D. C.

Chief of Naval Operations
Navy Dept.
ATTN: Cdr. R. Sherman, OP 754   64
Washington 25, D. C.

Commander
Ballistic Systems Division (AFSC)
ATTN: Capt. H. C. Tanner   65
Norton Air Force Base
California

Commander
Air Force Flight Dynamics Laboratory
ATTN: Mr. F. Adams   66
        Mr. F. Janik   67
        Capt. S. Garner   68
Air Force Systems Command
Wright-Patterson Air Force Base
Ohio

36

Commander
Air Force Weapon Laboratory
Air Research & Development Command
ATTN: WLX (Tech Dir AFWL)   69
            Maj. R. Smith   70
            WLAX   71
            Capt. Gillespie   72
            Lt. Col. R. Pennington   73
Kirtland Air Force Base
Albuquerque, New Mexico

Director
Lawrence Radiation Laboratory
P. O. Box 808
Livermore, California   74

Sandia Corporation
ATTN: Technical Library   75
P. O. Box 969
Livermore, California

Sandia Corporation
Sandia Base
ATTN: Classified Library   76
Albuquerque, New Mexico

RAND Corporation
1700 Main Street
Santa Monica, California   77

Research Analysis Corporation
6935 Arlington Road
Bethesda 14, Maryland   78

Defense Research Corporation
ATTN: Technical Library   79
4050 State Street
Santa Barbara, California

Institute for Defense Analysis
ATTN: Technical Library   80
1666 Connecticut Avenue, N. W.
Washington 9, D. C.

Aerospace Corporation
San Bernardino Operations
ATTN: D. Singer & A. Schmidt   81
P. O. Box 1308
San Bernardino, Calif.

Space Technology Labs
ATTN: Technical Library   82
1 Space Park
Redondo Beach, Calif.

Bell Telephone Laboratories
ATTN: Dr. D. Ling & Dr. F. Benedict   83
Whippany, N. J.

Kaman Aircraft Corporation
Kaman Nuclear Division
ATTN: J. P. Hoffman   84
Garden of the Gods Road
Colorado Springs, Colorado

Technical Operations Research
ATTN: Dr. P. Richards   85
Burlington, Massachusetts

Vitro Laboratories
West Orange Laboratory
ATTN: J. Baer   86
200 Pleasant Valley Way
West Orange, N. J.

Commanding Officer
Picatinny Arsenal
Dover, N. J.

ATTN:		Copy No.
	Director, Feltman Research Laboratories	87
	Chief, Engineering Sciences Laboratory	88
	Technical Assistant for Nuclear Effects	89
	Technical Assistant for Physics	90
	Chief, Nuclear Effects Section	91
	Director, Nuclear Engineering Directorate	92
	Chief, Nuclear Weapons Development Division	93
	Chief, Nuclear Systems Branch	94
	Chief, Vulnerability Branch	95